

Siberian Branch of Russian Academy of Science
BUDKER INSTITUTE OF NUCLEAR PHYSICS

G. Fiksel,, D.J. Den Hartog,
A.A. Ivanov, A.A. Lizunov

CALCULATION OF THE OPTICAL
TRANSITION INTENSITY
AND ENERGY LEVEL SPLITTING
FOR GENERAL CONDITIONS
OF THE MOTIONAL STARK EFFECT
DIAGNOSTIC

Budker INP 2003-29

Novosibirsk
2003

**Calculation of the optical transition intensity
and energy level splitting for general conditions
of the Motional Stark Effect diagnostic**

A.A. Ivanov, A.A. Lizunov

Budker Institute of Nuclear Physics
630090, Novosibirsk, SB RAS

D.J. Den Hartog, G. Fiksel

Department of Physics
University of Wisconsin-Madison, WI. 53706, USA

Abstract

The model of translational Stark splitting for the hydrogen Balmer-alpha line has been developed, which includes also fine structure effects and Zeeman splitting. The primary field of application is numerical modeling of spectra obtained in experiments in magnetic plasma confinement devices directed to measurement of low magnetic fields. The results of calculation for Balmer-alpha multiplet pattern are presented for typical conditions of experiments in the Gas Dynamic Trap (BINP, Russia) and Madison Symmetric Torus (UW, USA).

1 Introduction

Diagnostics for measurements of magnetic field magnitude and pitch-angle on the basis of a translational Stark effect (or Motional Stark Effect, MSE) are widely used in experiments in toroidal systems for magnetic plasma confinement [1], [2]. An MSE diagnostic has several obvious advantages, such as possibility to perform local measurements and capability of obtaining electric field value and direction in addition to \mathbf{B} measurements. Under typical conditions of experiments in tokamaks (magnetic field $1 \div 5$ T, beam energy $50 \div 100$ keV), the resulting splitting of the beam emission line due to the motional Stark effect is about two or three orders of magnitude larger than the fine structure of atom levels allowing to easily neglect the latter. Zeeman splitting becomes comparable to the MSE-driven one only at relatively low beam energies ~ 5 keV for magnetic field in the order of a few Tesla. Accordingly, a relatively simple model of intensity distribution in the recorded spectrum is applicable for measurements processing [3]. On the contrary, a proper interpretation of the measured spectrum in low-field MSE experiments requires the Zeeman splitting and fine structure to be taken into account. For example, the fine structure splitting of energy levels of a hydrogen atom amounts to $\approx 10\%$ of the splitting due to MSE for the beam energy 40 keV and magnetic field 2 kGs.

The present work has been pursued to allow for a proper interpretation of local measurements of $|B|$ in plasma in GDT experiment [4] at Budker Institute and magnetic field profile in MST device [5]. The magnetic field in both devices is relatively low, so that all the above mentioned splitting mechanisms are significant. The described numerical model allows to directly simulate an experimental spectrum of the Balmer alpha transition of a hydrogen atom for the real conditions of measurements. Similar calculations for H_α multiplet can be found in [6].

The paper is organized like follows. First in the section 2 the method of calculation of levels splitting and line intensities is discussed. Section 3 consistently states the construction of the perturbation Hamiltonian, which includes relevant effects. Also the limitations of the model applicability and approximations made are discussed in this section. Section 4 shows the results of calculation for various parameters including the typical conditions of MSE

experiments in GDT mirror device and Madison Symmetrical Torus. The conclusion at the end of the section summarizes results presented in the paper and considers possible application fields for the described model.

2 Method of calculations

As it is widely known (see, e.g. [7]), in the absence of external fields and neglecting relativistic effects, a hydrogen atom energy level with the momentum quantum number l is $(2l + 1)(2s + 1)$ times degenerated according to all possible directions of the momentum vector and spin $s = 1/2$ in space. Next order approximation should take into account relativistic effects in interaction between the electron and nucleus field. Strictly speaking, in this case the orbital momentum \mathbf{l} and spin \mathbf{s} are not conserved separately. Only law of conservation of the full momentum $\mathbf{j} = \mathbf{l} + \mathbf{s}$ remains as it is consequence of space isotropy with respect to a closed system. Spin-orbital coupling and other relativistic effects then can be taken into account as perturbation leading to small corrections of level energies. Hence in the first-order perturbation theory one can assume the absolute values (not projections) of \mathbf{l} and \mathbf{s} conserved and levels can be characterized by corresponding quantum numbers l and s . Arising of the external magnetic field leads to the breaking of degeneracy with regard to orbital momentum projection (Zeeman effect). Interaction of the atom electron with external electric field also breaks the levels degeneracy. The corresponding terms of the total perturbation Hamiltonian are studied in detail in Section 3.

It is convenient to work in $|l, s, m_l, m_s\rangle$ representation, which is defined by orthogonal set of electron eigenfunctions with given l, s, m_l, m_s - respectively the orbital quantum number, spin ($1/2$), z-projection of the orbital momentum and spin z-projection. In this representation interaction operators mentioned above have simple forms which can be easily derived. The wavefunction of a single electron in the spherically symmetric electrostatic potential of the hydrogen nucleus can be found in [7]. It has the following form:

$$|l, s, m_l, m_s\rangle = R_{nl} \cdot Y_l^{m_l} \cdot \mathbf{S}, \quad (1)$$

where R_{nl} is the radial part of the wavefunction, $Y_l^{m_l}$ is the spherical harmonic defining the angular part and \mathbf{S} is the Pauli spinor; $\begin{pmatrix} 1 \\ 0 \end{pmatrix}$ corresponds to the state with $m_s = 1/2$ and $\begin{pmatrix} 0 \\ 1 \end{pmatrix}$ corresponds to the state with

$m_s = -1/2$. Radial and angular wavefunctions for $n = 2$ and $n = 3$ states are tabulated e.g. in [8].

The total perturbation operator is expressed as a sum of the interaction operators:

$$\hat{\mathbf{H}}_{total} = \hat{\mathbf{H}}_{Stark} + \hat{\mathbf{H}}_{Zeeman} + \hat{\mathbf{H}}_{rel}, \quad (2)$$

where the term $\hat{\mathbf{H}}_{rel}$ is responsible for the spin-orbital coupling and other relativistic effects. Each term in (2) is examined in Section 3.

The calculation scheme comprises the following steps:

1. Specification of the calculation geometry and parameters. Modeling of the H_α multiplet was performed using the geometry of real MSE experiments. Instead of calculation of intensity for π and σ spectrum components separately (as it is usually done), we calculated lines intensity with the experimentally observed polarization.
2. Calculation of the operator (2) eigenvalues for $n = 2$ and $n = 3$ states, which represents the splitted energy levels of the multiplet with given n . Since in most general case the level degeneracy is totally removed, there are eight different eigenvalues for the $n = 2$ level and eighteen – for the $n = 3$ level. Each eigenvector, which corresponds to given eigenvalue for $n = 3$, represents a set of coefficients giving the expression in the chosen $|l, s, m_l, m_s\rangle$ basis:

$$\psi = \sum_{i=0}^8 c_i |l, s, m_l, m_s\rangle_i, \quad (3)$$

and similarly for $n = 3$ levels. To study the dependence of level energies upon magnetic field, this procedure must be rerun with the different value set. Numerical approach to the eigenvalue task is more preferable than the theoretical one, since no additional assumptions and simplifications have to be made.

3. To obtain the H_α multiplet component intensities one has to calculate matrix elements of r_i (x, y, z coordinates) between levels with different n as $\langle i | r_i | j \rangle$, where $\langle i |$ and $| j \rangle$ are eigenfunctions with $n = 3$ and $n = 2$, respectively. Expression for a transition intensity comprises the coordinate matrix elements as described in Section 3.
4. The final step is simulate spectrum setting a finite broadening for each line of the multiplet. In real condition of MSE experiments the broadening arises from several sources: finite beam temperature and angular divergence, specific light collection solid angle of registration optics, etc.

3 Perturbation operator

3.1 The relativistic effects

Relativistic effects in interaction of an electron with electromagnetic field are described by the Dirac theory [9]. As the electron speed in a hydrogen atom $v/c \sim \alpha \ll 1$, the relativistic corrections to Hamiltonian can be obtained by means of perturbation theory. Expansion of the Dirac equation in power series of $\frac{1}{c}$ leads to the following form of the Hamiltonian of an electron in the external electric field \mathbf{E} (see [10]):

$$\hat{\mathbf{H}} = \frac{\hat{\mathbf{p}}^2}{2m} + e\Phi - \frac{\hat{\mathbf{p}}^4}{8m^3c^2} - \frac{e\hbar}{4m^2c^2}\boldsymbol{\sigma}[\mathbf{E}\hat{\mathbf{p}}] - \frac{e\hbar^2}{8m^2c^2}\text{div}\mathbf{E}, \quad (4)$$

where $\boldsymbol{\sigma}$ is the Pauli matrix. The last three terms in (4) are of the order of $\sim \frac{1}{c^2}$. The first of them is due to the relativistic kinetic energy dependence on electron impulse (i.e. it is the result of $\sqrt{\mathbf{p}^2 - m^2c^2} - mc^2$ expansion). The second term is responsible for the spin-orbital interaction. The third term is non-zero only at the origin of coordinate where the nucleus is located. It is significant for calculation of the energy level shift for states with $l=0$.

Substituting the expression $\mathbf{E} = \frac{e\mathbf{r}}{r^3}$ for the hydrogen nucleus electric field into the (4), one can easily obtain the following form for the perturbation operator:

$$\hat{\mathbf{V}} = -\frac{\hat{\mathbf{p}}^4}{8m^3c^2} + \frac{1}{2}\left(\frac{e\hbar}{mc}\right)^2\frac{1}{r^3}\hat{\mathbf{I}}\hat{\mathbf{s}} + \frac{\pi e^2}{2\hbar c^3 m^2}\delta(\mathbf{r}). \quad (5)$$

Due to the spin-orbital interaction (the second term in (5)), an electron wavefunction becomes an eigenfunction of operators of full momentum squared $\hat{\mathbf{j}}^2 = (\hat{\mathbf{I}} + \hat{\mathbf{s}})^2$ and \hat{j}_z - z-projection of $\hat{\mathbf{j}}$. Accordingly, it gives rise to a new set of quantum numbers: j, m_j , which are eigenvalues of the corresponding operators. However, the levels with given n and j are still remain double-degenerated with regard to the orbital quantum number l : $l = j \pm 1/2$ [7, 10], except the levels with the maximal value of j for a given main quantum number n : $j_{max} = l_{max} + 1/2 = n - 1/2$. Each of the eigenfunction $|j, m_j\rangle$ is the superposition of two states with the same j but different l : $l = j \pm s$. These $|l, s, j, m_j\rangle$ states (Pauli eigenfunctions) can be in turn expressed in $|l, s, m_l, m_s\rangle$ representation as [7]

$$\mathbf{1} = \mathbf{j} - \frac{\mathbf{1}}{2} :$$

$$\begin{aligned} |j, m_j\rangle &= \sqrt{\frac{l+1/2+m_j}{2l+1}} |l, m_l = m_j - \frac{1}{2}, m_s = \frac{1}{2}\rangle \\ &- \sqrt{\frac{l+1/2-m_j}{2l+1}} |l, m_l = m_j + \frac{1}{2}, m_s = -\frac{1}{2}\rangle, \end{aligned}$$

$$\mathbf{1} = \mathbf{j} + \frac{\mathbf{1}}{2} :$$

$$\begin{aligned} |j, m_j\rangle &= \sqrt{\frac{l+1/2-m_j}{2l+1}} |l, m_l = m_j - \frac{1}{2}, m_s = \frac{1}{2}\rangle \\ &+ \sqrt{\frac{l+1/2+m_j}{2l+1}} |l, m_l = m_j + \frac{1}{2}, m_s = -\frac{1}{2}\rangle. \end{aligned}$$

The set of wavefunctions $|l, s, j, \bar{m}_j\rangle$ for $n = 2$ is written below:

$$\mathbf{1} = \mathbf{0} :$$

$$j = \frac{1}{2} :$$

$$|j = \frac{1}{2}, m_j = \frac{1}{2}\rangle = |0, \frac{1}{2}, 0, \frac{1}{2}\rangle,$$

$$|j = \frac{1}{2}, m_j = -\frac{1}{2}\rangle = |0, \frac{1}{2}, 0, -\frac{1}{2}\rangle,$$

$$\mathbf{1} = \mathbf{1} :$$

$$j = \frac{3}{2} :$$

$$|j = \frac{3}{2}, m_j = \frac{3}{2}\rangle = |1, \frac{1}{2}, 1, \frac{1}{2}\rangle,$$

$$|j = \frac{3}{2}, m_j = \frac{1}{2}\rangle = \sqrt{\frac{2}{3}} |1, \frac{1}{2}, 0, \frac{1}{2}\rangle - \sqrt{\frac{1}{3}} |1, \frac{1}{2}, 1, -\frac{1}{2}\rangle,$$

$$|j = \frac{3}{2}, m_j = -\frac{1}{2}\rangle = \sqrt{\frac{1}{3}} |1, \frac{1}{2}, -1, \frac{1}{2}\rangle - \sqrt{\frac{2}{3}} |1, \frac{1}{2}, 0, -\frac{1}{2}\rangle,$$

$$|j = \frac{3}{2}, m_j = -\frac{3}{2}\rangle = |1, \frac{1}{2}, -1, -\frac{1}{2}\rangle.$$

$$\begin{aligned}
j = \frac{1}{2} & : \\
|j = \frac{1}{2}, m_j = \frac{1}{2}\rangle &= \sqrt{\frac{1}{3}}|1, \frac{1}{2}, 0, \frac{1}{2}\rangle + \sqrt{\frac{2}{3}}|1, \frac{1}{2}, 1, -\frac{1}{2}\rangle, \\
|j = \frac{1}{2}, m_j = -\frac{1}{2}\rangle &= \sqrt{\frac{2}{3}}|1, \frac{1}{2}, -1, \frac{1}{2}\rangle + \sqrt{\frac{1}{3}}|1, \frac{1}{2}, 0, -\frac{1}{2}\rangle.
\end{aligned}$$

The set of wavefunctions $|l, s, j, m_j\rangle$ for $n = 3$ can be written in the same way:

$$\begin{aligned}
\mathbf{1} = \mathbf{2} & : \\
j = \frac{5}{2} & : \\
|j = \frac{5}{2}, m_j = \frac{5}{2}\rangle &= |2, \frac{1}{2}, 2, \frac{1}{2}\rangle, \\
|j = \frac{5}{2}, m_j = \frac{3}{2}\rangle &= \sqrt{\frac{4}{5}}|2, \frac{1}{2}, 1, \frac{1}{2}\rangle - \sqrt{\frac{1}{5}}|2, \frac{1}{2}, 2, -\frac{1}{2}\rangle, \\
|j = \frac{5}{2}, m_j = \frac{1}{2}\rangle &= \sqrt{\frac{3}{5}}|2, \frac{1}{2}, 0, \frac{1}{2}\rangle - \sqrt{\frac{2}{5}}|2, \frac{1}{2}, 1, -\frac{1}{2}\rangle, \\
|j = \frac{5}{2}, m_j = -\frac{1}{2}\rangle &= \sqrt{\frac{2}{5}}|2, \frac{1}{2}, -1, \frac{1}{2}\rangle - \sqrt{\frac{3}{5}}|2, \frac{1}{2}, 0, -\frac{1}{2}\rangle, \\
|j = \frac{5}{2}, m_j = -\frac{3}{2}\rangle &= \sqrt{\frac{1}{5}}|2, \frac{1}{2}, -2, \frac{1}{2}\rangle - \sqrt{\frac{4}{5}}|2, \frac{1}{2}, -1, -\frac{1}{2}\rangle, \\
|j = \frac{5}{2}, m_j = -\frac{5}{2}\rangle &= |2, \frac{1}{2}, -2, -\frac{1}{2}\rangle.
\end{aligned}$$

$$\begin{aligned}
j = \frac{3}{2} & : \\
|j = \frac{3}{2}, m_j = \frac{3}{2}\rangle &= \sqrt{\frac{1}{5}}|2, \frac{1}{2}, 1, \frac{1}{2}\rangle + \sqrt{\frac{4}{5}}|2, \frac{1}{2}, 2, -\frac{1}{2}\rangle, \\
|j = \frac{3}{2}, m_j = \frac{1}{2}\rangle &= \sqrt{\frac{2}{5}}|2, \frac{1}{2}, 0, \frac{1}{2}\rangle + \sqrt{\frac{3}{5}}|2, \frac{1}{2}, 1, -\frac{1}{2}\rangle, \\
|j = \frac{3}{2}, m_j = -\frac{1}{2}\rangle &= \sqrt{\frac{3}{5}}|2, \frac{1}{2}, -1, \frac{1}{2}\rangle + \sqrt{\frac{2}{5}}|2, \frac{1}{2}, 0, -\frac{1}{2}\rangle, \\
|j = \frac{3}{2}, m_j = -\frac{3}{2}\rangle &= \sqrt{\frac{4}{5}}|2, \frac{1}{2}, -2, \frac{1}{2}\rangle + \sqrt{\frac{1}{5}}|2, \frac{1}{2}, -1, -\frac{1}{2}\rangle.
\end{aligned}$$

The $n = 3$ states also includes the $3P_{3/2}$, $3P_{1/2}$ and $3S_{1/2}$ wavefunctions, corresponding to momentum quantum numbers $l = 1$ and $l = 0$. These wavefunctions are identical to the corresponding $n = 2$ states. Averaging of the perturbation operator (5) over state $|n, j\rangle$ leads to the well known equation

$$\Delta\varepsilon = -\frac{m\alpha^4}{2n^3} \left(\frac{1}{j+1/2} - \frac{3}{4n} \right), \quad (6)$$

which contains relativistic corrections of the order $1/c^2$, as it is discussed above. Taking into account (6), the energy for a hydrogen atom states are defined by the formula (see [10, 7])

$$E_{nj} = -\frac{Ry}{n^2} \left[1 + \frac{\alpha^2}{n} \left(\frac{1}{j+1/2} - \frac{3}{4n} \right) \right]. \quad (7)$$

In equations (6), (7) Ry is the wave number corresponding to the energy unity in Rydberg, α is the fine structure constant. The values of physical constants used in the calculation are tabulated in Section 5 for helper purposes.

The remaining double degeneracy of levels $|j, m_j\rangle$ with regard to an orbital momentum l disappears due to radiation corrections or Lamb shift [11], which are not taken into account by the single-electron Dirac equation. In the first order perturbation theory only s -state (with $l = 0$) undergoes the Lamb shift, which can be calculated using the formula (see [7]):

$$\Delta E_n^{Lamb} = \frac{8\alpha^3}{3\pi n^3} Ry \left[2 \ln \frac{1}{\alpha} + \ln \frac{Ry}{K_0(n)} + \frac{19}{30} \right], \quad (8)$$

where $K_0(2)/Ry = 16.64$, $K_0(3)/Ry = 15.921$.

The corrections to (7) of the next order given by subsequent terms of Hamiltonian (5) are $\sim \alpha \cdot \Delta E_n^{Lamb}$ and can be therefore neglected. Finally the fine structure energies can be calculated including the Lamb shift of the $2S$ and $3S$ states. Assuming the $2S_{1/2}$ and $3S_{1/2}$ state energies equal to zero for convenience, fine structure energies for $n = 2$ are: ¹

$$\begin{aligned} E_0 &= E(2S_{1/2}) = 0, \\ E_1 &= E(2P_{1/2}) = -0.035279 \text{ cm}^{-1}, \\ E_3 &= E(2P_{3/2}) = 0.330594 \text{ cm}^{-1}. \end{aligned}$$

¹Taken from the NIST database, <http://physics.nist.gov/cuu/Constants/index.html>

and similarly for $n = 3$:

$$\begin{aligned}
E_0 &= E(3S_{1/2}) = 0, \\
E_1 &= E(3P_{1/2}) = -0.010331 \text{ cm}^{-1}, \\
E_3 &= E(3P_{3/2}, 3D_{3/2}) = 0.097885 \text{ cm}^{-1} \\
E_5 &= E(3D_{5/2}) = 0.133957 \text{ cm}^{-1}.
\end{aligned}$$

3.2 Zeeman effect

Our consideration of the interaction between the electron magnetic dipole and external magnetic field is limited to the first order perturbation theory. This simplification, however, does not reduce any significantly the applicability of the model for simulation of H_α multiplet measured in plasma MSE experiments. The second order of the perturbation theory, which is responsible for the quadratic Zeeman effect, is much less than fine structure splitting for magnetic fields ≤ 25 T.

Within the $|l, s, m_l, m_s\rangle$ representation, which is used in the paper, the linear Zeeman effect operator is represented by the diagonal matrix

$$\hat{\mathbf{H}}_{Zeeman} = (g_l \hat{\mathbf{L}}_z + g_s \hat{\mathbf{S}}_z) \mu_B B_z. \quad (9)$$

Here $\hat{\mathbf{L}}_z$ and $\hat{\mathbf{S}}_z$ are operators of orbital momentum and spin z-projection, μ_B is the Bohr magneton, g_l and g_s are g-factors of orbital momentum and spin, respectively. Factor g_l is unity according to the Dirac theory [9], value of g_s can be found in the Section 5.

3.3 Motional Stark effect

Stark effect is responsible for level splitting due to breaking of degeneracy of electron states for an atom in external electric field. For hydrogen and hydrogen-like atoms Stark splitting is linear effect, providing thus good base for diagnostic applications. In the frame of reference of a fast atom moving in external magnetic field B , the Lorenz electric field $\mathbf{E}_L = \frac{1}{c}[\mathbf{v} \times \mathbf{B}]$ appears, causing energy levels to split. Directions of the magnetic field, beam velocity and observation line defined in our calculation, are shown in Fig.1. This geometry models conditions of GDT experiment [12]. Polarization directions \mathbf{e}_1 and \mathbf{e}_2 (see Fig.1) correspond to observed ones.

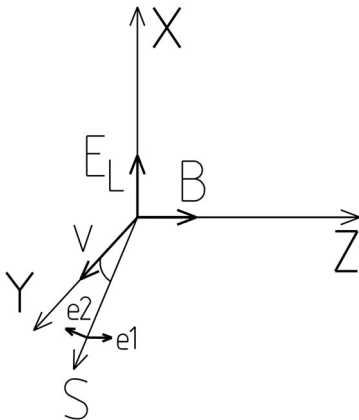


Figure 1: Geometry used in the calculation. B - magnetic field, v - hydrogen beam velocity, E_L - Lorenz electric field, S - direction of observation (in the xy -plane), e_1 and e_2 - two independent polarization of emitted radiation ($e_1 \parallel z$).

The term in the perturbation Hamiltonian (4) responsible for the motional Stark effect, has the following form [7]:

$$\hat{H}_{Stark} = \frac{evB}{c} \cdot \hat{x}. \quad (10)$$

Matrix elements of (10) in $|l, s, m_l, m_s\rangle$ representation are given by integrals

$$\langle n, 1/2, m_l, m_s | x | n, \acute{l}, 1/2, \acute{m}_l, \acute{m}_s \rangle = x_{n, \acute{l}, m_l}^{n, \acute{l}, \acute{m}_l} \cdot \delta_{m_s}^{\acute{m}_s}, \quad (11)$$

multiplied by the constant $\frac{evB}{c}$. Integrals (11) with $n = 2$ form the operator matrix 8×8 elements for the lower state of the multiplet, the operator matrix for $n = 3$ (upper) state has 18×18 elements. Separating (11) into radial and angular parts, one obtains:

$$x_{n, \acute{l}, m_l}^{n, \acute{l}, \acute{m}_l} = \int_0^\pi P_{\acute{l} \acute{m}_l}(\theta) P_{lm}(\theta) \cos \theta \sin \theta d\theta \times \int_0^{2\pi} \frac{1}{2\pi} e^{i(m_l - \acute{m}_l)\varphi} \frac{e^{i\varphi} + e^{-i\varphi}}{2} d\varphi \cdot R_{n, \acute{l}}^{n, \acute{l}}. \quad (12)$$

Here radial integrals are:

$$R_{n,l}^{n,l} = \int_0^\infty R_{n_l}(r)R_{n_l}(r)r^3 dr. \quad (13)$$

Since (11) and all other matrix elements, which are considered in respect to our calculation are diagonal by m_s index, it will be omitted below. It is most convenient to calculate (11) using conventional definitions of linear combinations

$$D_+ = x + iy = r \sin \theta \cdot e^{i\varphi},$$

$$D_- = x - iy = r \sin \theta \cdot e^{-i\varphi}.$$

Matrix elements of D_\pm can be written as follows [7]:

$$\begin{aligned} (x + iy)_{n,l,m_l}^{n,l+1,m_l+1} &= \sqrt{\frac{(l+m_l+2)(l+m_l+1)}{(2l+3)(2l+1)}} R_{n_l}^{n,l+1}, \\ (x - iy)_{n,l,m_l}^{n,l+1,m_l-1} &= -\sqrt{\frac{(l-m_l+2)(l-m_l+1)}{(2l+3)(2l+1)}} R_{n_l}^{n,l+1}, \\ (x + iy)_{n,l,m_l}^{n,l-1,m_l+1} &= -\sqrt{\frac{(l-m_l)(l-m_l-1)}{(2l+1)(2l-1)}} R_{n_l}^{n,l-1}, \\ (x - iy)_{n,l,m_l}^{n,l-1,m_l-1} &= \sqrt{\frac{(l+m_l)(l+m_l-1)}{(2l+1)(2l-1)}} R_{n_l}^{n,l-1}. \end{aligned} \quad (14)$$

All others matrix elements are zero. Hence we get the following selection rules for the l and m_l : $\Delta l = \hat{l} - l = \pm 1$, $\Delta m_l = \hat{m}_l - m_l = \pm 1$. According to [7], radial integrals can be calculated as

$$R_{n,l}^{n,l-1} = R_{n,l-1}^{n,l} = \frac{3}{2} a_0 n \sqrt{n^2 - l^2}, \quad (15)$$

where a_0 is the Bohr radius. Matrix elements of x can be now easily calculated as

$$x_{n_l m_l}^{n_l \hat{m}_l} = \frac{1}{2} [(x + iy)_{n_l m_l}^{n_l \hat{m}_l} + (x - iy)_{n_l m_l}^{n_l \hat{m}_l}].$$

3.4 Complete perturbation Hamiltonian

Combining (5), (9) and (10), we get Hamiltonian (4) in the form

$$\begin{aligned}\hat{\mathbf{H}} &= -\frac{\hat{\mathbf{p}}^4}{8m^3c^2} + \frac{1}{2} \left(\frac{e\hbar}{mc} \right)^2 \frac{1}{r^3} \hat{\mathbf{l}}\hat{\mathbf{s}} + \frac{\pi e^2}{2\hbar c^3 m^2} \delta(\mathbf{r}) \\ &+ (g_l \hat{\mathbf{L}}_z + g_s \hat{\mathbf{S}}_z) \mu_B B_z \\ &+ \frac{evB}{c} \cdot \hat{x}\end{aligned}\quad (16)$$

Matrices of the operator (16) in the $|l, s, m_l, m_s\rangle$ representation for $n = 2$ and $n = 3$ levels are presented in Section 6. Theoretical solution of eigenvalue problem for (16) is not possible in most general case. The set of eigenvalues and eigenvectors was computed for given values of beam velocity and magnetic field by diagonalizing the matrices.

3.5 Calculation of the H_α multiplet component intensities

Intensity of the optical transition $\acute{n} \longrightarrow n$ for radiation with polarization \mathbf{e} in erg/sec-ster is given by the formula (see [7]):

$$J_e = \frac{e^2}{2\pi c^3} \omega^4 (\mathbf{e} \mathbf{r}_{\acute{n}n})^2, \quad (17)$$

where $\omega = (E_{\acute{n}} - E_n)/\hbar$ is the radiation frequency, $\mathbf{r}_{\acute{n}n}$ – the dipole matrix element:

$$\mathbf{r}_{\acute{n}n} = \int \psi_{\acute{n}}^* \sum \mathbf{r}_i \psi_n d\tau, \quad (18)$$

where the integral is taken over the configuration space of the atom electron. For polarization directions \mathbf{e}_1 and \mathbf{e}_2 used in the calculation (see Fig.1) we obtain intensity as

$$\begin{aligned}J_{e_1} &= \frac{e^2}{2\pi c^3} \omega^4 |z_{\acute{n}n}|^2, \\ J_{e_2} &= \frac{e^2}{2\pi c^3} \omega^4 (|x_{\acute{n}n}|^2 + |y_{\acute{n}n}|^2).\end{aligned}\quad (19)$$

Upper and lower states of the transition $\acute{n} \longrightarrow n$ are the eigenfunctions of the perturbation operator (16):

$$\begin{aligned}
|\acute{n}\rangle &= \sum_{\acute{l}, \acute{m}_l} a_{\acute{l}\acute{m}_l} |3, \acute{l}, \frac{1}{2}, \acute{m}_l\rangle, \\
|n\rangle &= \sum_{l, m_l} b_{lm_l} |2, l, \frac{1}{2}, m_l\rangle,
\end{aligned} \tag{20}$$

where coefficients $a_{\acute{l}\acute{m}_l}$ and b_{lm_l} in linear expansions (20) in term of used $|l, s, m_l, m_s\rangle$ basis are components of eigenvectors corresponding to the states of $|\acute{n}\rangle$ and $|n\rangle$. Thus coordinate matrix elements can be written as

$$\begin{aligned}
x_{\acute{n}n} &= \sum \sum a_{\acute{l}\acute{m}_l}^* b_{lm_l} \langle 2, l, 1/2, m_l | x | 3, \acute{l}, 1/2, \acute{m}_l \rangle, \\
y_{\acute{n}n} &= \sum \sum a_{\acute{l}\acute{m}_l}^* b_{lm_l} \langle 2, l, 1/2, m_l | y | 3, \acute{l}, 1/2, \acute{m}_l \rangle, \\
z_{\acute{n}n} &= \sum \sum a_{\acute{l}\acute{m}_l}^* b_{lm_l} \langle 2, l, 1/2, m_l | z | 3, \acute{l}, 1/2, \acute{m}_l \rangle.
\end{aligned} \tag{21}$$

Matrix elements for x and y -coordinate can be evaluated according to the equations

$$\begin{aligned}
x_{\acute{n}n} &= \frac{1}{2} [(x + iy)_{\acute{n}n} + (x - iy)_{\acute{n}n}], \\
y_{\acute{n}n} &= -\frac{i}{2} [(x + iy)_{\acute{n}n} - (x - iy)_{\acute{n}n}].
\end{aligned}$$

Here matrix elements for $x \pm iy$ for transitions between the $|l, s, m_l, m_s\rangle$ states are written as in (14), but the upper and lower states in radial integrals are \acute{n} and n . For further considerations it is convenient to write also the equations for matrix elements of z -coordinate (see [7]):

$$\begin{aligned}
z_{\acute{n}lm_l}^{\acute{n}l+1m_l} &= \sqrt{\frac{(l+1)^2 - m_l^2}{(2l+3)(2l+1)}} R_{nl}^{\acute{n}l+1}, \\
z_{\acute{n}lm_l}^{\acute{n}l-1m_l} &= \sqrt{\frac{l^2 - m_l^2}{(2l+1)(2l-1)}} R_{nl}^{\acute{n}l-1},
\end{aligned} \tag{22}$$

and $z_{\acute{n}lm_l}^{\acute{n}l\acute{m}_l}$ are zero in all other cases.

Radial integrals from eqs. (14) and (22) are tabulated in [7]. Their expressions for a transition of the Balmer series are the following:

$$\begin{aligned}
 2s \longrightarrow np : R_{20}^{n1} &= \sqrt{\frac{2^{17}n^9(n^2-1)(n-2)^{2n-6}}{(n+2)^{2n+6}}}, \\
 2p \longrightarrow nd : R_{21}^{n2} &= \sqrt{\frac{2^{19}n^9(n^2-1)(n-2)^{2n-7}}{3(n+2)^{2n+7}}}, \\
 2p \longrightarrow ns : R_{21}^{n0} &= \sqrt{\frac{2^{15}n^9(n-2)^{2n-6}}{3(n+2)^{2n+6}}}.
 \end{aligned} \tag{23}$$

Equations (22) and (14) lead to the following selection rules: $\Delta m_l = \pm 1$, $\Delta l = \pm 1$ for transitions with e_2 polarization (magnetic dipole) and $\Delta m_l = 0$, $\Delta l = \pm 1$ for transitions with e_1 polarization (electric dipole). In other words, if $\langle \hat{n}|z|n \rangle^2 \neq 0$, then both $\langle \hat{n}|x|n \rangle^2 = 0$ and $\langle \hat{n}|y|n \rangle^2 = 0$ (and vice versa).

4 Results of calculation

4.1 Consideration of the calculation verification

To provide the code verification, several additional calculations were performed. Oscillator strengths submit to the well-known Thomas-Reiche-Kuhn (TRK) sum rule (see [7]), which was utilized for the examination of dipole matrix elements (18) calculation. Also we have made a comparison of calculated energy levels with those tabulated in the NIST database.¹ Results of simulation of levels splitting and multiplet spectrum pattern were found to be in agreement with the results obtained in similar calculations by other authors [6].

4.2 Results of H_α multiplet modeling

This section shows the results of calculation of the H_α multiplet spectrum for typical conditions of motional Stark measurements in low-field devices for plasma confinement. Fig.2 presents the dependence of a hydrogen atom level splitting upon magnetic field. The relatively low beam velocity of 10^7 cm/s is set for this calculation to make the fine structure and translational Stark effect (and also "pure" Zeeman effect) similar in magnitude.

¹<http://physics.nist.gov>

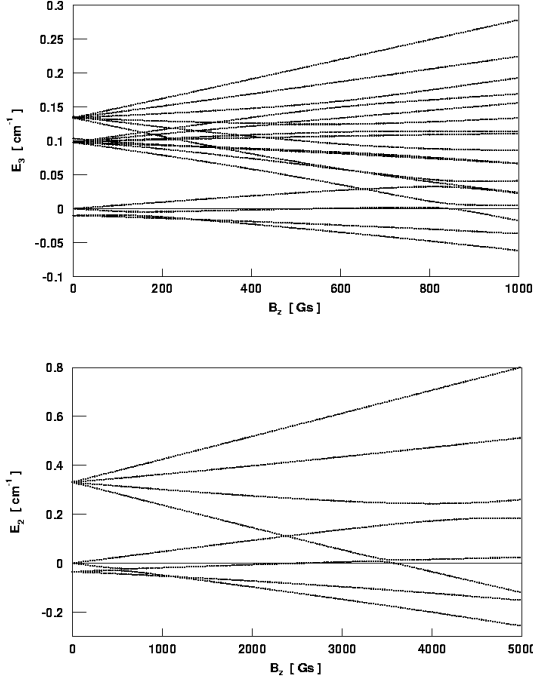


Figure 2: Calculated splitting of the $n = 3$ (upper plot) and $n = 2$ (lower plot) levels as a function of the magnetic field strength.

In most works devoted to spectrum calculations, π and σ polarizations of emitted radiation are considered separately [6]. However, in general case of real experiment, radiation with mixed polarization is observed. In the present paper the geometry in Fig.1 is used. Accordingly, intensity of radiation with the polarization \mathbf{e}_2 is $J_{e_2} = J_\pi \cos^2 \Theta + J_\sigma \sin^2 \Theta$, where Θ is the angle between the beam and viewing line (see Fig.1). Polarization \mathbf{e}_1 in this case is equal to π_B polarization, i.e. it is parallel to the magnetic field.

Fig.3 presents the calculated spectrum for 40 keV hydrogen beam moving in magnetic field of 4 kGs, where the observation angle Θ is set to 22.5° . These values are close to parameters typical for the GDT experiment [12]. Since level degeneracy is completely removed, the model spectrum comprises 144 separate lines, corresponding to transitions from 18 levels $n = 3$ to 8

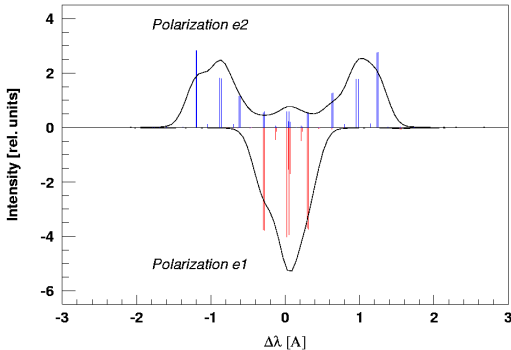


Figure 3: The spectrum of the H_α multiplet for beam energy 40 keV and magnetic field 4 kGs. Lines with e_1 polarization are plotted in the negative direction of Y axis for convenience. Curves in the plot show the model spectrum assuming a finite broadening for each line.

levels with $n = 2$. Stark effect alone would result in equidistant splitting with the spacing between component proportional to the magnetic field. Fine structure of levels differ this pattern as it is seen in Fig.3. This effect is more sharply demonstrated in Fig.4. The spectrum was calculated for the following diagnostic parameters: beam energy 40 keV, magnetic field 2 kGs, observation angle $\Theta = 22.5^\circ$. Obviously, application of the simple motional Stark splitting model for processing spectra obtained in experiment under similar conditions, would result in considerable error.

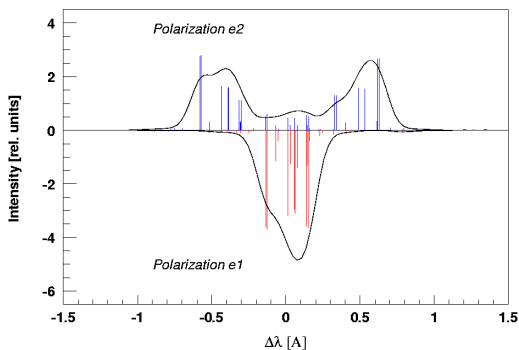


Figure 4: The spectrum of the H_α multiplet for beam energy 40 keV and magnetic field 2 kGs.

Fig.5 shows calculated H_α spectrum for beam energy 30 keV and magnetic field 4 kGs, which are typical parameters of MSE measurements in MST [5].

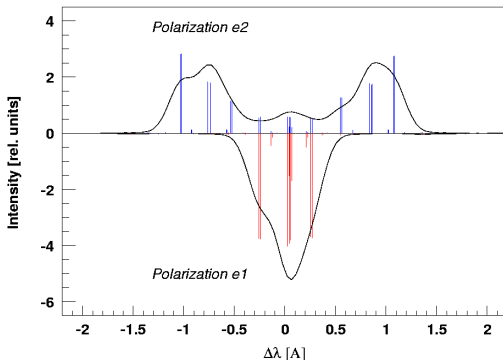


Figure 5: The spectrum of the H_α multiplet for beam energy 30 keV and magnetic field 4 kGs.

4.3 Summary

The code based on the combined Stark, Zeeman and fine structure splitting, has been developed allowing for calculation of H_α multiplet spectra in general condition of MSE experiment. Geometry used for calculations is shown in Fig.1. However, it can be flexibly changed enabling adaptation for a wider field of application. Mainly, the purpose of the model is processing of spectra obtained in low-field (magnetic field ≤ 4 kGs) spectroscopic measurements of $|\mathbf{B}|$. Some spectra are presented showing the importance of including all the mentioned splitting mechanisms for achievement of the reliable modeling result. The model can be also used for data processing in tokamak MSE measurements for increasing of the accuracy.

We did not consider in the work the effects of internal electric fields in the plasma, where diagnostic hydrogen beam propagates. Oscillating electric fields could differ the static spectrum structure only for slow particles (thermal with the temperature of few eV). Such fields $E \sim 10^3$ V/cm could be developed by plasma instabilities. Quasi-static electric field in plasma can be measured using the same spectroscopic technique [1, 2]. Described model is planned to be further upgraded in order to enable simulation of combined measurements.

5 Physical constants used in the paper

For helper purposes, this section contains the list of fundamental physical constants used for calculation. Values are taken from the National Institute of Standards and Technology (NIST) database. ¹

- Light speed $c = 2.99792458 \cdot 10^{10}$ cm/s,
- Electron mass $m_e = 9.10938188 \cdot 10^{-28}$ g,
- Proton mass $1.67262158 \cdot 10^{-24}$ g,
- Electron charge $e = 4.8065293860 \cdot 10^{-10}$ statcoul,
- Planck constant $\hbar = 1.054571596 \cdot 10^{-27}$ erg·s,
- Bohr radius $a_0 = 0.5291772083 \cdot 10^{-8}$ cm,
- Bohr magneton $\mu_B = 927.400899 \cdot 10^{-23}$ erg·Gs,
- Fine structure constant $\alpha = 7.297352533 \cdot 10^{-3}$,
- Inverse fine structure constant $\alpha^{-1} = 137.03599976$,
- Rydberg constant $Ry = 109737.31568549$ cm,
- Electron spin g-factor $g_s = 2.0023193043737$,
- Conversion factor $1 \text{ cm}^{-1} = 1.98644544 \cdot 10^{-16}$ erg.

Next Section 6 contains the matrices of perturbation Hamiltonian (16) in the $|l, s, m_l, m_s\rangle$ representation for $n = 2$ and $n = 3$ states. Values of fine structure energies E_1, E_3 for $n = 2$ levels and E_1, E_3, E_5 for $n = 3$ levels can be found in the Section 3.

In the matrix for $n = 3$, E_s is the "Stark" energy: $E_s = e\mathbf{E}_L \cdot a_0$, where \mathbf{E}_L is the Lorentz electric field, a_0 is the Bohr radius.

¹The URL is <http://physics.nist.gov/cuu/Constants/index.html>

6 Hamiltonian matrices

The perturbation Hamiltonian (16) matrix for $n = 2$ states is shown below.

m_l		0	0	1	1	1	0	0	0	-1	-1
	m_s	$1/2$	$-1/2$	$1/2$	$1/2$	$-1/2$	$1/2$	$1/2$	$-1/2$	$1/2$	$-1/2$
0	$1/2$	$E_0 + \frac{g_s^s B \mu_B}{2}$	0	$\frac{3}{\sqrt{2}} \frac{e v B}{c} a_0$	0	0	0	0	0	$-\frac{3}{\sqrt{2}} \frac{e v B}{c} a_0$	0
0	$-1/2$	0	$E_0 - \frac{g_s^s B \mu_B}{2}$	0	$\frac{3}{\sqrt{2}} \frac{e v B}{c} a_0$	0	0	0	0	0	$-\frac{3}{\sqrt{2}} \frac{e v B}{c} a_0$
1	$1/2$	$\frac{3}{\sqrt{2}} \frac{e v B}{c} a_0$	0	$E_3 + \frac{g_s^s B \mu_B}{2}$	$E_3 + \frac{g_s^s B \mu_B}{2}$	0	0	0	0	0	0
1	$-1/2$	0	$\frac{3}{\sqrt{2}} \frac{e v B}{c} a_0$	0	$\frac{2}{3} E_1 + \frac{1}{3} E_3 + \frac{\sqrt{2}}{3} (E_3 - E_1)$	$(g_l - \frac{g_s^s}{2}) B \mu_B$	$\frac{2}{3} E_1 + \frac{1}{3} E_3 + \frac{\sqrt{2}}{3} (E_3 - E_1)$	0	0	0	0
0	$1/2$	0	0	0	$\frac{1}{3} E_1 + \frac{2}{3} E_3 + \frac{g_s^s B \mu_B}{2}$	$(g_l + \frac{g_s^s}{2}) B \mu_B$	$\frac{1}{3} E_1 + \frac{2}{3} E_3 + \frac{g_s^s B \mu_B}{2}$	0	0	0	0
0	$-1/2$	0	0	0	$\frac{1}{3} E_1 + \frac{2}{3} E_3 - \frac{g_s^s B \mu_B}{2}$	$(g_l - \frac{g_s^s}{2}) B \mu_B$	$\frac{1}{3} E_1 + \frac{2}{3} E_3 - \frac{g_s^s B \mu_B}{2}$	$\frac{\sqrt{2}}{3} (E_3 - E_1)$	$\frac{\sqrt{2}}{3} (E_3 - E_1)$	0	0
-1	$1/2 - \frac{3}{\sqrt{2}} \frac{e v B}{c} a_0$	$\frac{3}{\sqrt{2}} \frac{e v B}{c} a_0$	0	0	0	0	0	0	0	$\frac{2}{3} E_1 + \frac{1}{3} E_3 - (-g_l + \frac{g_s^s}{2}) B \mu_B$	0
-1	$-1/2$	0	$-\frac{3}{\sqrt{2}} \frac{e v B}{c} a_0$	0	0	0	0	0	0	0	$E_3 - (g_l + \frac{g_s^s}{2}) B \mu_B$

Since scaling the 18×18 element matrix in order to fit the A4 page makes it almost unreadable, the matrix for $n = 3$ states is divided into four blocks:

A	C
C	B

Each block is a square matrix 9×9 .

Block A.

m_l		0	0	1	1	1	0	0	0	-1	-1	2
	m_s	$1/2$	$-1/2$	$1/2$	$-1/2$	$1/2$	$1/2$	$-1/2$	$-1/2$	$1/2$	$-1/2$	$1/2$
0	$1/2$	$\frac{g_s}{2} B\mu_B$	0	$3\sqrt{3}E_s$	0	0	0	0	$-3\sqrt{3}E_s$	0	0	0
0	$-1/2$	0	$-\frac{g_s}{2} B\mu_B$	0	$3\sqrt{3}E_s$	0	0	0	0	$-3\sqrt{3}E_s$	0	0
1	$1/2$	$3\sqrt{3}E_s$	0	$E_3 + (g_l + \frac{g_s}{2})B\mu_B$	0	0	0	0	0	0	0	$\frac{9}{2}E_s$
1	$-1/2$	0	$3\sqrt{3}E_s$	0	$\frac{2}{3}E_1 + \frac{1}{3}E_3 + (g_l - \frac{g_s}{2})B\mu_B$	$\frac{\sqrt{2}}{3}(E_3 - E_1)$	0	0	0	0	0	0
0	$1/2$	0	0	0	$\frac{2}{3}E_3 + \frac{1}{3}E_1 + \frac{g_s}{2}B\mu_B$	0	0	0	0	0	0	0
0	$-1/2$	0	0	0	0	0	0	$\frac{2}{3}E_3 + \frac{1}{3}E_1 - \frac{g_s}{2}B\mu_B$	$\frac{\sqrt{2}}{3}(E_3 - E_1)$	0	0	0
-1	$1/2$	$-3\sqrt{3}E_s$	0	0	0	0	0	0	$\frac{2}{3}E_1 + \frac{1}{3}E_3 + (-g_l + \frac{g_s}{2})B\mu_B$	0	0	0
-1	$-1/2$	0	$-3\sqrt{3}E_s$	0	0	0	0	0	0	$E_3 - (g_l + \frac{g_s}{2})B\mu_B$	0	0
2	$1/2$			$\frac{9}{2}E_s$	0	0	0	0	0	0	0	$E_5 + (2g_l + \frac{g_s}{2})B\mu_B$

Block B (next page).

Block C (values of m_l and m_s correspond to the lower left block).

m_l		0	0	1	1	0	0	-1	-1	2
	m_s	1/2	-1/2	1/2	-1/2	1/2	-1/2	1/2	-1/2	1/2
2	-1/2	0	0	0	$\frac{9}{2}E_s$	0	0	0	0	0
1	1/2	0	0	0	0	$\frac{9}{2\sqrt{2}}E_s$	0	0	0	0
1	-1/2	0	0	0	0	0	$\frac{9}{2\sqrt{2}}E_s$	0	0	0
0	1/2	0	0	$-(\frac{3}{2})^{3/2}E_s$	0	0	0	$(\frac{3}{2})^{3/2}E_s$	0	0
0	-1/2	0	0	0	$-(\frac{3}{2})^{3/2}E_s$	0	0	0	$(\frac{3}{2})^{3/2}E_s$	0
-1	1/2	0	0	0	0	$-\frac{9}{2\sqrt{2}}E_s$	0	0	0	0
-1	-1/2	0	0	0	0	0	$-\frac{9}{2\sqrt{2}}E_s$	0	0	0
-2	1/2	0	0	0	0	0	0	$-\frac{9}{2}E_s$	0	0
-2	-1/2	0	0	0	0	0	0	0	$-\frac{9}{2}E_s$	0

References

- [1] F. Levington *Rev. Sci. Instr.*, vol. 70, p. 810, Jan. 1999.
- [2] T. Soetens, R. Jaspers, and E. Desoppere *Rev. Sci. Instr.*, vol. 70, p. 890, Jan. 1999.
- [3] W. Mandl, R. Wolf, M. von Hellerman, and H. Summers *Plasma Physics and Controlled Fusion*, vol. 35, p. 1737, 1993.
- [4] A. Ivanov, A. Anikeev, P. Bagryansky, A. Karpushov, S.A.Korepanov, V. Kornilov, A. Lizunov, V. Maximov, and S. Murakhtin in *Transaction of Fusion Technology*, vol. 39, p. 127, 2001.
- [5] R. Dexter, D. Kerst, T. Lovell, S. Prager, and J. Sprott, "The madison symmetric torus," *Fusion Tech.*, vol. 19, p. 131, 1991.
- [6] E. Souw and J. Uhlenbusch *Physica*, vol. 122C, p. 353, 1983.
- [7] H. Bete and C. Salpeter, *Quantum Mechanics of One and Two Electron Atoms*. New York: Plenum Press, 1977.
- [8] B. Smirnov, *Fizika atoma i iona*. Energoatomizdat, 1986. In russian.
- [9] P. Dirac, *The Principles of Quantum Mechanics*. Oxford: Oxford Science Publications, 4th ed., March 1982.
- [10] V. Berestetskij, E. Lifshitz, and L. Pitaevskij, *Quantum electrodynamics*. Elsevier Science, January 1982.
- [11] W. Lamb *Rep. Progr. Physics*, vol. 14, p. 19, 1951.
- [12] P. Bagryansky, D. Den Hartog, G. Fiksel, A. Ivanov, S. Korepanov, A. Lizunov, and V. Savkin in *Proc. 28th EPS Conference on Contr. Fusion and Plasma Phys., Funchal, 18-22 June 2001, ECA*, vol. 25A, p. 1217, 2001.